A gain-of-function TBX20 mutation causes congenital atrial septal defects, patent foramen ovale and cardiac valve defects

Maximilian G Posch,[1] Michael Gramlich,[2] Margaret Sunde,[3] Katharina R Schmitt,[4] Stella H Y Lee,[2] Silke Richter,[1] Andrea Kersten,[1] Andreas Perrot,[1] Anna N Panek,[1] Iman H Al Khatib,[5] Georges Nemer,[5] André Mégarbané,[6] Rainer Dietz,[1] Brigitte Stiller,[7] Felix Berger,[4] Richard P Harvey,[2,8] Cemil Özcelik[1]

[1]Experimental and Clinical Research Center (ECRC), Charité - Universitätsmedizin, Berlin, Germany
[2]Victor Chang Cardiac Research Institute, Darlinghurst, New South Wales, Australia
[3]School of Molecular and Microbial Biosciences, University of Sydney, New South Wales 2006, Australia
[4]Department for Congenital Heart Disease and Paediatric Cardiology, Charite - Universitätsmedizin Berlin and German Heart Institute Berlin, Germany
[5]Department of Biochemistry, American University of Beirut (AUB), Beirut, Lebanon
[6]Department of Medical Genetics, Faculty of Medicine, St. Joseph University, Beirut, Lebanon
[7]Department for Paediatric Cardiology, University of Freiburg, Freiburg, Germany
[8]Faculties of Medicine and Science, University of New South Wales, Kensington, New South Wales, Australia

Correspondence to
Dr Maximilian Posch, ECRC, Lindenberger Weg 80, 13125 Berlin, Germany;
maximilian.posch@charite.de

Maximilian G Posch, Michael Gramlich, and Margaret Sunde contributed equally to this work.

Received 2 June 2009
Revised 27 July 2009
Accepted 17 August 2009

ABSTRACT

Background Ostium secundum atrial septal defects (ASDII) account for approximately 10% of all congenital heart defects (CHD), and mutations in cardiac transcription factors, including *TBX20*, were identified as an underlying cause for ASDII. However, very little is known about disease penetrance in families and functional consequences of inherited TBX20 mutations.

Methods The coding region of *TBX20* was directly sequenced in 170 ASDII patients. Functional consequences of one novel mutation were investigated by surface plasmon resonance, CD spectropolarymetry, fluorescence spectrophotometry, luciferase assay and chromatin immunoprecipitation.

Results We found a novel mutation in a highly conserved residue in the T-box DNA binding domain (I121M) segregating with CHD in a three generation kindred. Four mutation carriers revealed cardiac phenotypes in terms of cribriform ASDII, large patent foramen ovale or cardiac valve defects. Interestingly, tertiary hydrophobic interactions within the mutant TBX20 T-box were significantly altered leading to a more dynamic structure of the protein. Moreover, Tbx20-I121M resulted in a significantly enhanced transcriptional activity, which was further increased in the presence of co-transcription factors GATA4/5 and NKX2-5. Occupancy of DNA binding sites on target genes was also increased.

Conclusions We suggest that TBX20-I121M adopts a more fluid tertiary structure leading to enhanced interactions with cofactors and more stable transcriptional complexes on target DNA sequences. Our data, combined with that of others, suggest that human ASDII may be related to loss-of-function as well as gain-of-function TBX20 mutations.

INTRODUCTION

Congenital heart defects (CHD) occur in approximately 1% of all newborns and are the most common developmental error in humans. Ostium secundum atrial septal defects (ASDII) account for approximately 10% of all CHD. Genetic mutations have been identified as an underlying cause for familial recurrence of ASDII in humans.[1] Most disease genes encode cardiac transcription factors and show autosomal dominant inheritance with incomplete disease penetrance. Cardiac transcription factor genes *NKX2-5* and *GATA4* are the most extensively studied for non-syndromic CHD (MIM 600584 and MIM 600576). Thus far, pathogenicity of CHD related transcription factor mutations is mainly explained by partial or complete loss of function resulting in hypomorphic transcriptional activity.[2–4] The most prevalent clinical phenotype found in probands with transcription factor mutations is ASDII. Correspondingly, ASDII is the type of CHD whose familial recurrence is most extensively documented (MIM 607941).[5]

T-box genes encode a family of highly conserved transcription factors that play a crucial role in organ development.[6] Genetic mutations in TBX1 and TBX5 are linked to clinical syndromes also involving the heart (MIM 188400 and MIM 142900).[7 8] TBX20 is an ancient member of the T-box superfamily highly expressed in embryonic heart tissues. Genetic ablation of TBX20 causes failure in cardiac growth and morphogenesis, and embryonic death at mid-gestation.[9] Mutations in human TBX20 were first reported in two family pedigrees with a spectrum of ASDII, cardiac valve defects and cardiomyopathy (MIM 611363).[10] Recently, several missense variants in TBX20 have also been noted in Chinese and American patients with various CHD, although functional analysis and family studies to establish pathological status have not been performed.[11 12] To assess the prevalence of TBX20 mutations in patients with ASDII, we sequenced the coding regions of TBX20 in 170 ASDII probands and studied the functional consequences of a novel missense mutation in a highly conserved T-box region.

PATIENTS AND METHODS

Study population and mutational analysis and molecular modelling

One hundred and seventy patients with ASDII attended the Department for Pediatric Cardiology at the German Heart Institute Berlin and gave written informed consent. Control subjects (n=340) underwent echocardiography to exclude CHD. In addition 218 ethnically matched control probands from two clinical centres in Lebanon were genotyped to exclude TBX20-I121M. Coding region of TBX20 (NM_020417) was amplified as described[10] and polymerase chain reaction (PCR) fragments were directly sequenced. The study was approved by the Institutional Review Board of the Charité and conforms to the Declaration of

Helsinki. The homology model of the TBX20 T-box domain was produced using the protein structure homology modelling server SWISS-MODEL[13] and based on the structure of the T-box domain of human TBX3 (PDB 1h6f).[14]

Mutagenesis, transfection and transcriptional assays

Full length cDNA expression constructs for wild-type (WT) mouse TBX20a and c, TBX20-I152M, TBX20-Q195X, NKX2-5, GATA4 and GATA5 as well as the luciferase reporter vectors pANF-700-Luc and pGL3-Gja5 have been described previously.[10 15] The I121M mutation was introduced into pCDNA3.1-Tbx20a/c by PCR based, site directed mutagenesis and confirmed by sequencing. COS7 cells were transfected with expression and reporter vectors using Lipofectamine. CMV-renilla luciferase reporter vector was used as a control for the transfection efficacy. Cells were harvested after 24 h and luciferase activity was measured using the Dual-Luciferase Reporter 1000 assay system (Promega, Madison, Wisconsin, USA). Transcription data are listed as average±SEM, representing three independent transfections, each done in triplicate. Statistical analysis was performed using the Student t test.

Biophysical studies

The T-box domains were expressed as fusion proteins as previously described.[13] Circular dichroism (CD) data were recorded on a Jasco J-720 spectropolarimeter equipped with a Neslab RTE-111 temperature controller as described.[11 13] Surface plasmon resonance kinetic analysis was performed on a Biacore 2000 SPR instrument. Pairs of oligonucleotides (CTCTAGTCACACCTAGGTGTGAAATT (*T-site*) and CTCTTATAGGTGTGAAAACCGTG (*T/2*), with one partner containing a 5′-biotin group, were immobilised on a streptavidin coated SA sensor chip following the manufacturer's protocol. Binding of ANS (1-anilinonapthalene-8-sulfonic acid) was analysed with protein at 0.18 mg/ml and ANS at 0.1 mg/ml at pH 7.4. ANS fluorescence was measured in a Varian CARY Eclipse Fluorescence spectrophotometer with a temperature controlled cell.

Chromatin immunoprecipitation (ChIP) and quantitative PCR

COS7 cells were grown overnight in 150 mm dishes to 70% confluency and then co-transfected with the pANF-Luc reporter vector and expression vectors for TBX20a (WT, I121M, I152M), Nkx2-5 and Gata4. After 24 h, cells were cross-linked with formaldehyde, harvested and immunoprecipitations were performed essentially as described previously.[16] Antibodies used in this procedure include TBX20 (Orbigen, Inc, California, USA), NKX2-5 (Santa Cruz Biotechnology, Inc, California, USA) and rabbit IgG. The bound DNA was analysed by semiquantitative PCR with primers for the *Nppa* promoter (forward 5′-GAGCGCCCAGGAAGATAACCA-3′; reverse 5′-AGTGACA-GAATGGGGAGGGTTCT-3′) and the endogenous Hprt promoter region as a negative control (forward 5′-GGCAGCGTTTCTGAGCCA-3′; reverse 5′- AAAGCAGT-GAGGTAAGCCCAAC-3′). Real-time PCR was carried out using the LightCycler 480 DNA SYBR Green I Master mix on a LightCycler 480 (Roche Applied Science, Mannheim, Germany) with primers for the *Nppa* promoter and *Gapdh* for normalisation. Fold enrichment relative to WT TBX20 was calculated using the comparative CT method (ΔΔCT method). Experiments were repeated at least three times.

RESULTS

One heterozygous C→G transversion at position c.374 (NM_020417) was detected in a 16-year-old male subject of Lebanese origin with ASDII (figure 1A). The variant results in a shift from isoleucine to methionine in the TBX20 protein (I121M) and was not found among 680 control alleles. We also screened 218 control probands from Lebanon but found no TBX20-I121M, excluding it as an ethnically restricted polymorphism. The affected residue lies in the T-box DNA binding region and is highly conserved among species (figure 1B). Two in silico tools (PolyPhen and SIFT)[17 18] predicted functional consequences for the variant. As shown in figure 2 the residue of Ile121 packs between side chains of Arg127 and Tyr267, which make important interactions with DNA.[14] To investigate disease segregation in the family pedigree, we characterised relatives of the proband (figure 1C). The index patient (IV:4) had a cribriform ASDII with three distinct perforations in the atrial septum. The proband's grandmother (II:2) was reported to suffer from combined cardiac valve defects and underwent surgical replacement of aortic and mitral valves at age 35. She died at age 55 and no DNA was available. However, genotyping of proband III:1 and his half-sister (III:2) indicated that II:2 was most likely also harbouring I121M (figure 1C). Subject III:1 declined clinical characterisation but consented to genetic analysis. The proband's mother (III:2) and sister (IV:2) showed large patent foramen ovale (PFO) with permanent shunt as seen in transoesophageal echocardiography. Both were positive for the mutation. Subjects III:3, IV:1 and IV:3 had no atrial shunts or other echocardiographic abnormalities and did not harbour the mutation.

To scrutinise alterations in structural stability of I121M we used CD spectropolarimetry. Figure 3A shows that the I121M

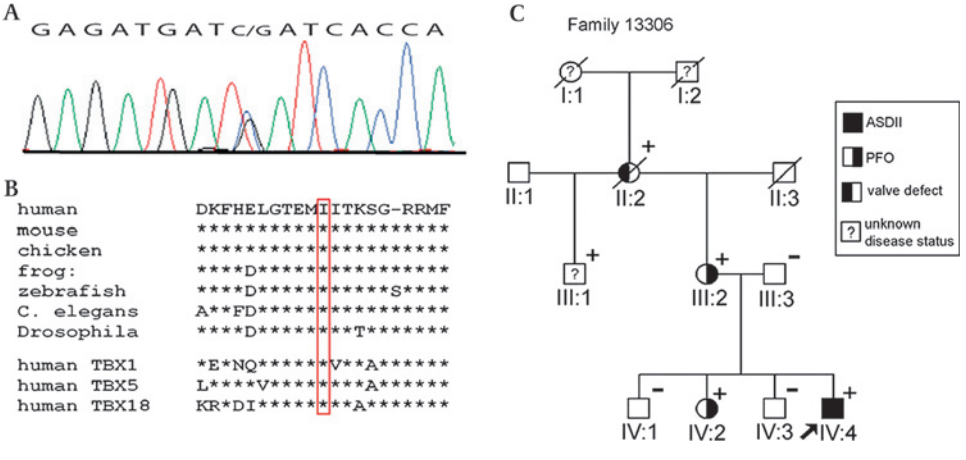

Figure 1 (A) The relevant sequence electropherogram of TBX20 (NM_020417) exon 2 in the proband. (B) The affected amino acid (Ile121) lies in a highly conserved N-terminal region of the DNA binding T-box region of TBX20. Affected region of TBX20 homologues and human TBX paralogues are shown. (C) Family pedigree of mutation carriers. The proband is marked with an arrow. All subjects which were genotyped for TBX20-I121M are indicated with + (carrier) or − (non-carrier). Subject II:2 was presumed positive for TBX20-I121M (plus symbol in parentheses) as indicated by the genotypes of progeny (III:1 and III:2).

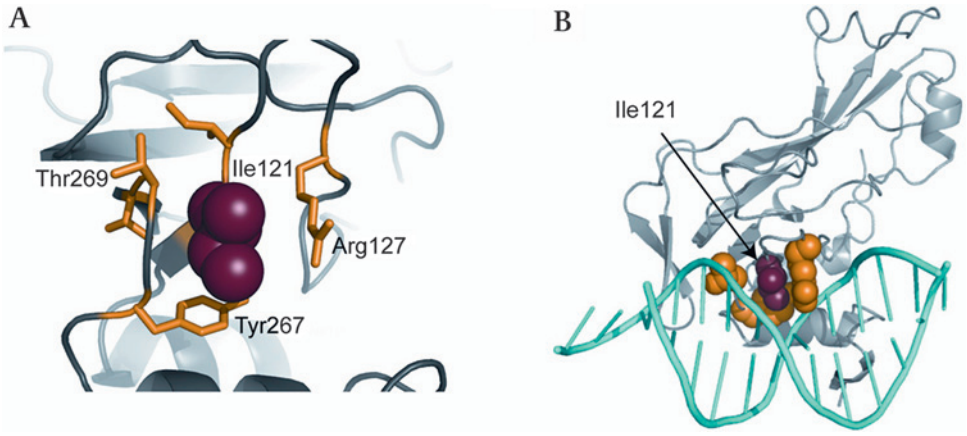

Figure 2 (A) The homology model of TBX20, based on the structure of human TBX3, suggests that the side chain of Ile121 packs between the side chains of Arg127 and Tyr267 and adjacent to Thr269. (B) In TBX3, the residues equivalent to Arg127 and Tyr267 (Arg130 and Tyr264) make important interactions with the DNA, making it possible that changes at residue 121 might affect the binding of the T-box to DNA.

T-box was folded into a predominantly β-sheet structure, virtually identical to that of the WT domain at 20°C. Thermal denaturation of secondary structure in the mutant protein, monitored as loss of CD ellipticity signal at 215 nm, demonstrated that the melting temperature of I121M T-box was approximately 2°C lower than that of the WT T-box (figure 3B). We also probed the tertiary structure of the mutant domain using binding of ANS, a hydrophobic fluorescent molecule that displays enhanced fluorescence when surrounded by non-polar amino acids in proteins. While both WT and TBX20–I121M T-boxes displayed increased ANS binding at 37°C relative to 20°C, the I121M mutant showed a significantly greater fluorescence shift than WT TBX20 at the higher temperature (figure 3D). The mutation therefore appears to destabilise both secondary structure, albeit only weakly, and tertiary structural interactions within the hydrophobic core of the T-box domain, resulting in a conformation that has a more dynamic tertiary structure than the WT protein.

To assess structural features further, we measured DNA binding affinity of the mutant T-box. EMSA on transfected cells proved to be too insensitive to quantify subtle DNA binding changes in the context of the full length protein. We therefore measured the DNA binding kinetics of bacterially expressed recombinant T-box protein on the T-half site or T-site DNA sequences by surface plasmon resonance. The affinity of the I121M mutant T-box for the binding sites at 20°C was not significantly changed ($1.83\pm0.33\times10^{-6}$ M for I121M vs $1.24\pm0.27\times10^{-6}$ M for WT) (figure 3C). Attempts to measure the DNA binding affinity at 37°C failed because prolonged incubation of the I121M T-box at this temperature led to aggregation and irreversible binding to the sensor chip.

We next tested transcriptional activity of mutant and WT TBX20 using luciferase assays. The long isoform of WT TBX20 (TBX20a) has weak intrinsic transcriptional activity, likely because of the dominant effects of its C-terminal repression domain.[15] However, strong synergistic transcriptional potential in

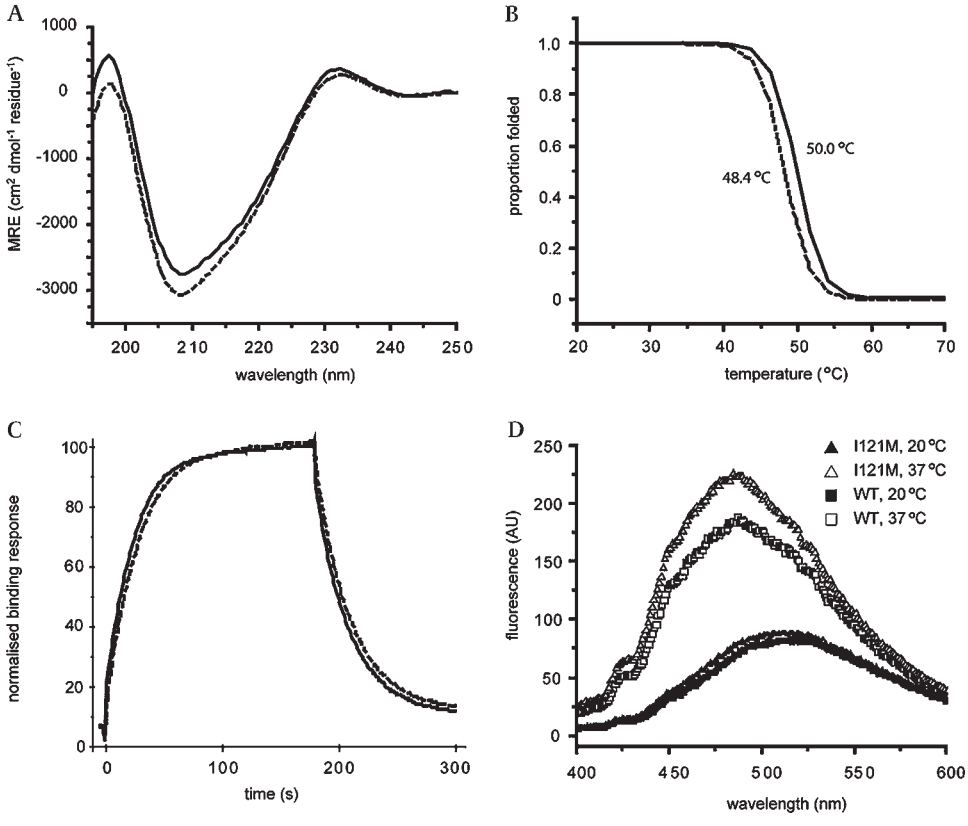

Figure 3 Biophysical characterisation of the I121M variant T-box. (A) Far UV CD spectra of WT (solid line) and I121M variant (dashed line) TBX20 T-box domains indicate similar folded, β-sheet rich secondary structures. (B) Proportion of secondary structure folded as protein is heated. The I121M variant (dashed line) domain displays a ~2°C reduction in T_m compared to WT (solid line), as measured by loss of CD signal at 215 nm. (C) Binding curves for I121M (dashed line) and WT (solid line) from representative surface plasmon resonance kinetic experiment. The mutation does not significantly affect the affinity of the domain for the T-site, as evidenced by very similar rates for binding and dissociation from the DNA displayed by both domains. (D) ANS fluorescence measured for I121M at 20°C and 37°C (solid and open triangles, respectively) and WT TBX20 T-box at 20 and 37°C (solid and open squares, respectively). Both domains show increased ANS binding at 37°C, a sign that tertiary contacts are relatively weak but the variant binds more ANS than the WT domain, indicating that the mutation destabilises the hydrophobic core further.

TBX20a is revealed when it is expressed with interacting transcription factors NKX2-5 and GATA4 (*Nppa* promoter[10]) or NKX2-5 and GATA4 (*Gja5* promoter[15]). The short TBX20 isoform (TBX20c) lacks the C-terminal repression and activation domains, and shows a higher baseline activity when overexpressed. TBX20c-I121M alone induced significantly higher activation of both the *Nppa* and *Gja5* enhancers compared to WT TBX20c (23% and 99%, respectively, p=0.01/0.04; figure 4A,C). A similar result was seen when the I121M mutation was introduced into the human TBX20 cDNA (data not shown). The increased activity of the mutant was even more apparent in the presence of NKX2-5 and GATA4/5 for both target genes (*Nppa*: 162%, p=0.01; *Gja5*: 127%, p=0.004; figure 4B,D). In contrast, previously identified TBX20 nonsense mutation Q195X resulted in reduced transcriptional activity, while the mis-sense mutation I152M, which showed reduced DNA binding on-rate, also displayed a gain-of-function transcriptional activity in some assays.[10]

To obtain further insight into these gain-of-function properties of I121M, we tested the occupancy of TBX20 WT and mutant proteins, and NKX2-5, on respective DNA binding sites within the *Nppa* enhancer in transfected COS7 cells by ChIP. Immunoprecipitation of cross-linked DNA/protein complexes with a TBX20 or NKX2-5 antibody, followed by semi-quantitative (figure 5A) and real-time PCR (figure 5B), revealed significantly enhanced occupancy of the I121M, on the Nppa promoter. In contrast the previously identified ASDII mutation I152M, which showed decreased DNA binding,[10] also displayed decreased occupancy. NKX2-5 revealed enhanced occupancy in the presence of TBX20-I121M and decreased occupancy with the TBX20-I152M mutation.

DISCUSSION

We describe a novel mutation in TBX20 associated with CHD in a kindred spanning three generations. The cardiac phenotypes of TBX20-I121M carriers are of particular interest: the proband harbouring I121M had a multiperforated atrial septum—a cribriform ASDII. During embryonic development, the septum primum grows from the primordial atrial roof towards the

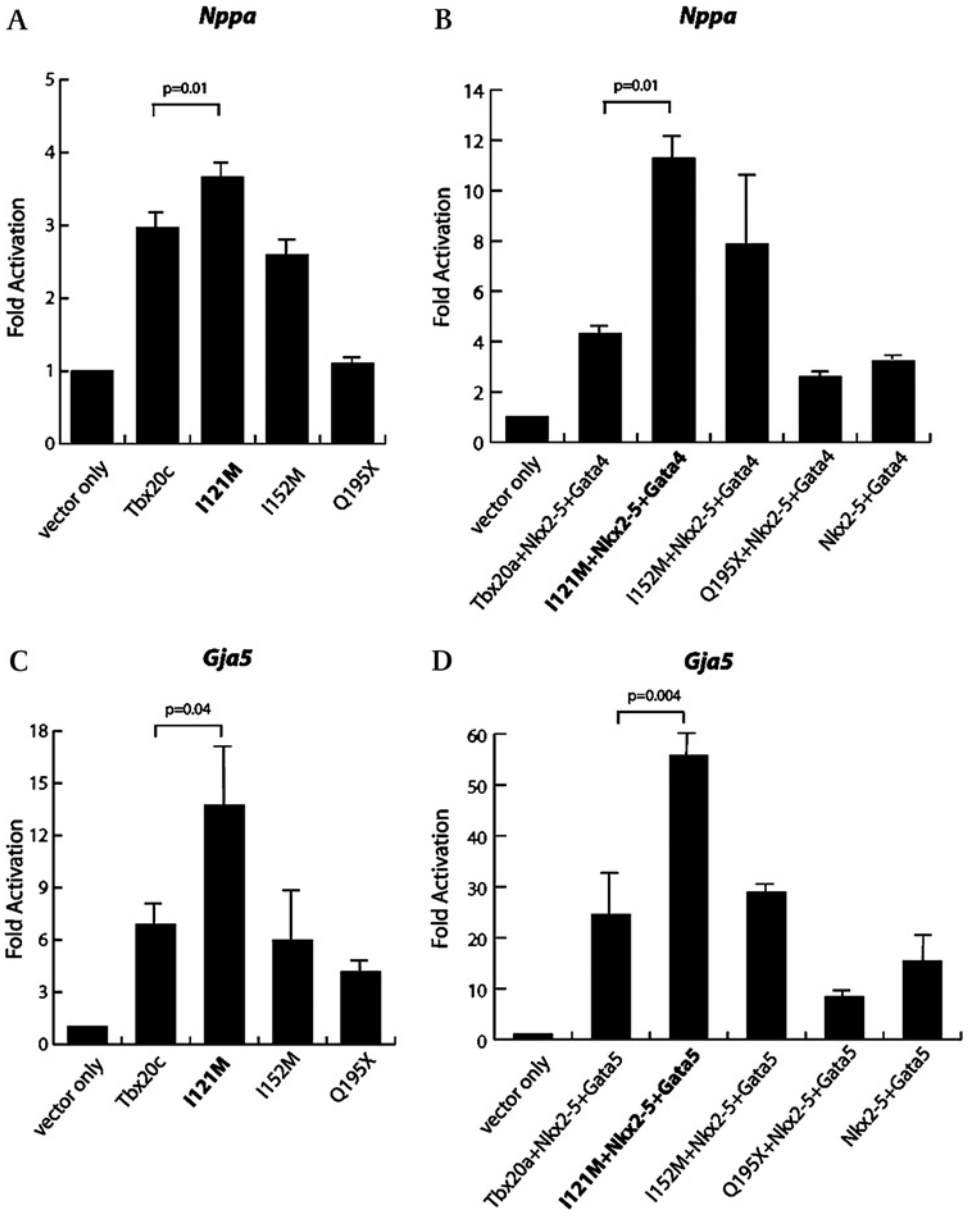

Figure 4 Transcriptional activity of WT and mutated TBX20 (I121M) and of the previously published TBX20 mutations I152M and Q195X. (A) Fold activation of a luciferase reporter construct carrying the proximal promoter elements of the *Nppa* gene after cotransfection of COS7 cells with expression constructs for WT and mutant TBX20 (short isoform). (B) Activation of the *Nppa* promoter in the presence of mutant and WT TBX20a (full length isoform), NKX2-5 and GATA4. (C, D) Fold activation of a luciferase reporter carrying proximal promoter elements of the *Gja5* gene.

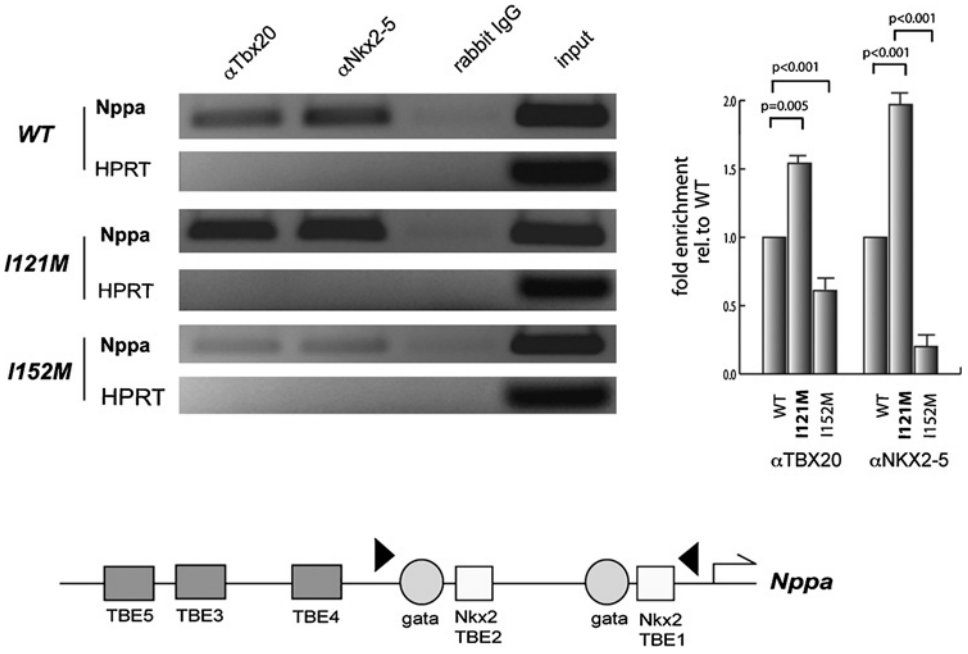

Figure 5 Immunoprecipitation assay with transiently transfected COS7 cells using an antibody against TBX20 and NKX2-5, followed by semiquantitative and real-time PCR reveals an enhanced occupancy of the Nppa promoter. Fold enrichment relative to WT Tbx20 was calculated using the comparative CT method. HPRT unrelated negative control; Rabbit IgG: negative control antibody. Lower panel: schematic diagram of the proximal Nppa promoter indicating the positions of T-box, GATA, and Nkx2 factor binding sites. The positions of the primers used for the ChIP analysis are indicated as arrowheads.

endocardial cushion. Simultaneously, small perforations develop in the upper part of the septum primum as a result of cell death, which coalesce with each other to form the foramen secundum. Cribriform ASDII are the result of an incomplete mergence of these perforations as well as an insufficient growth of the septum secundum. Interestingly, we and others have previously identified cribriform ASDII as a cardiac phenotype in patients with mutations in NKX2-5 and GATA4.[19 20] Thus, one may hypothesise that cribriform ASDII is overrepresented among patients with genetic ASDII and can result from perturbations to multiple individual transcription factors acting within an interactive regulatory network controlling atrial septation. The cardiac phenotypes of the proband's relatives were convergent with clinical features in patients harbouring the presumed TBX20 loss-of-function mutation Q195X,[10] confirming a crucial role for normal levels of TBX20 activity in human atrial septation and valvulogenesis. Two I121M carriers (III:2 and IV:2) had so far undiagnosed atypically large PFOs accompanied by a permanent left to right shunt. These findings are also in accordance with patients harbouring different mutations in TBX20.[10 11] PFOs derive from incomplete adhesion of the septum primum to the septum secundum after birth, leaving a functional communication between both atria via oblique, slit shaped tunnels. PFOs have a prevalence of approximately 30% in the general population. However, large PFOs with a defect of 10 mm or more as noted in the two TBX20-I121M carriers are found in only 1.3% of the population.[21] Human family studies strongly indicate familial clustering of PFO and ASD, especially those with larger defects and atrial shunts.[22 23] However, very little is known about genetic defects related to human PFO. Studies with inbred mice carrying heterozygous *Nkx2-5* mutations reveal defects in atrial septal morphogenesis resulting in ASDII as well as PFO, the latter depending on atrial morphological characteristics including length of the septum primum.[24] Quantitative trait loci analyses in different mouse strains strongly support the notion of an anatomic continuum between secundum ASD and PFO.[25] Notably, TBX20 overlaps with one such suggestive QTL (unpublished data Richard P Harvey, 2006).

An interesting finding of the present study was the mutation related gain-of-function. In contrast to most previously characterised CHD associated mutations, Tbx20-I121M showed significantly enhanced transcriptional activity of two target genes. Enhanced activity was even more pronounced when TBX20-I121M was co-expressed with NKX2-5 and GATA4/5. Importantly, I121M also showed enhanced occupancy of Nppa promoter DNA in transfected cells in the ChIP. These properties were observed in the absence of effects on DNA binding (albeit measured at 20°C) and the secondary structure of the mutant T-box was only slightly less thermally stable than that of the WT. However, tertiary packing in the hydrophobic core was significantly weakened by the mutation. The tertiary structure of the WT TBX20 T-box is far less thermally stable than that of parologous factors TBX5 and TBX2. Indeed, TBX20 therefore has unique biophysical characteristics compared to other cardiac T-box proteins in that it populates a molten globule state at 37°C.[13] The I121M mutant T-box displayed an even more dynamic tertiary structure than the WT T-box. While enhanced occupancy of target promoters could in principal be related to enhanced DNA binding, this was not observed and there are other possibilities, such as an enhanced rate of scanning of DNA or cofactors for interaction, or enhanced structural stability when bound to cofactors. The increased occupancy of NKX2-5 supports the idea of a more stable transcriptional complex and our data suggest that complex formation and/or stability is driven to a significant degree by transcription factor interactions, in this case between TBX20 and NKX2-5. Nevertheless, caution should be exercised in extrapolating the in vitro data to the in vivo situation. Though a significant gain-of-function was observed in multiple transcriptional assays, the protein might be less stable in vivo converging with a loss-of-function phenotype.

In vitro studies with CHD associated mutations in NKX2-5 and GATA4 revealed in most cases an impaired transactivation with either preserved or decreased DNA binding affinity.[2–4] It is therefore generally appreciated that haploinsufficiency of transcription is a common genetic root of CHD.[1] However, Postma and colleagues characterised a novel TBX5 missense mutation found in a family with atypical Holt Oram syndrome displaying enhanced transcription of several target genes associated with an increased DNA binding affinity.[26] Moreover, TBX20 was shown to be significantly upregulated in ventricular tissue from CHD

patients which may cause an increased activity in cardiomyocytes.[16] It is important to note, however, that the degree of relationship between functional consequences of gene mutations and specific anatomic findings remains highly speculative and additional genetic variants and environmental factors can influence clinical features of mutation carriers.

In conclusion, we have identified one novel missense variant in TBX20 associated with congenital atrial septal and cardiac valve defects resulting in unique biophysical properties compared to previously studied TBX20 mutations related to CHD. Notably, the mutation exhibited significantly increased transcriptional activity in vitro, as well as increased synergy with its cardiac co-transcription factors NKX2-5 and GATA4/5, and increased occupancy on the DNA of two target genes.

Acknowledgements The authors wish to thank the family for cooperation on this project. We sincerely thank Paul Vukašin for preparation of the GST-Tbx20-I121M variant T-box expression construct. This work was supported by the German Helmholtz Gemeinschaft (VH-VI 152), Deutsche Forschungsgemeinschaft (GR3411/1-11) and National Health and Medical Research Counsel, Australia (354400).

Competing interests None.

Ethics approval This study was conducted with the approval of the Charite, Berlin, Germany.

Patient consent Obtained.

Provenance and peer review Not commissioned; externally peer reviewed.

REFERENCES

1. **Bruneau BG.** The developmental genetics of congenital heart disease. *Nature* 2008;**451**:943—8.
2. **Garg V,** Kathiriya IS, Barnes R, Schluterman MK, King IN, Butler CA, Rothrock CR, Eapen RS, Hirayama-Yamada K, Joo K, Matsoka R, Cohen JC, Srivastava D. GATA4 mutations cause human congenital heart defects and reveal an interaction with TBX5. *Nature* 2003;**424**:443—7.
3. **Kasahara H,** Benson DW. Biochemical analyses of eight NKX2.5 homeodomain missense mutations causing atrioventricular block and cardiac anomalies. *Cardiovasc Res* 2004;**64**:40—51.
4. **Nemer G,** Fadlalah F, Usta J, Nemer M, Dbaibo G, Obeid M, Bitar F. A novel mutation in the GATA4 gene in patients with Tetralogy of Fallot. *Hum Mutat* 2006;**27**:293—4.
5. **Caputo S,** Capozzi G, Russo MG, Esposito T, Martina L, Cardaropoli D, Ricci C, Argiento P, Pacileo G, Calabro R. Familial recurrence of congenital heart disease in patients with ostium secundum atrial septal defect. *Eur Heart J* 2005;**26**:2179—84.
6. **Stennard FA,** Harvey RP. T-box transcription factors and their roles in regulatory hierarchies in the developing heart. *Development* 2005;**132**:4897—910.
7. **Basson CT,** Bachinsky DR, Lin RC, Levi T, Elkins JA, Soults J, Grayzel D, Kroumpouzou E, Traill TA, Leblanc-Straceski J, Renault B, Kucherlapati R, Seidman JG, Seidman CE. Mutations in human TBX5 cause limb and cardiac malformation in Holt-Oram syndrome. *Nat Genet* 1997;**15**:30—5.
8. **Yagi H,** Furutani Y, Hamada H, Sasaki T, Asakawa S, Ichida F, Joo K, Kimura M, Imamura S, Kamatani N, Momma K, Takao A, Nakazawa M, Shimizu N, Matsuoka R. Role of TBX1 in human del22q11.2 syndrome. *Lancet* 2003;**362**:1366—73.
9. **Stennard FA,** Costa MW, Lai D, Biben C, Furtado MB, Solloway MJ, McCulley DJ, Leimena C, Preis JI, Dunwoodie SL, Elliot DE, Prall OW, Black BL, Fatkin D, Harvey RP. Murine T-box transcription factor Tbx20 acts as a repressor during heart development, and is essential for adult heart integrity, function and adaptation. *Development* 2005;**132**:2451—62.
10. **Kirk EP,** Sunde M, Costa MW, Rankin SA, Wolstein O, Castro ML, Butler TL, Hyun C, Guo G, Otway R, Mackay JP, Waddell LB, Cole AD, Hayward C, Keogh A, Macdonald P, Griffiths L, Fatkin D, Sholler GF, Zorn AM, Feneley MP, Winlaw DS, Harvey RP. Mutations in cardiac T-box factor gene TBX20 are associated with diverse cardiac pathologies, including defects of septation and valvulogenesis and cardiomyopathy. *Am J Hum Genet* 2007;**81**:280—91.
11. **Liu C,** Shen A, Li X, Jiao W, Zhang X, Li Z. T-box transcription factor TBX20 mutations in Chinese patients with congenital heart disease. *Eur J Med Genet* 2008;**51**:580—7.
12. **Qian L,** Mohapatra B, Akasaka T, Liu J, Ocorr K, Towbin JA, Bodmer R. Transcription factor neuromancer/TBX20 is required for cardiac function in Drosophila with implications for human heart disease. *Proc Natl Acad Sci U S A* 2008;**105**:19833—8.
13. **Macindoe I,** Glockner L, Vukašin P, Stennard FA, Costa MW, Harvey RP, Mackay JP, Sunde M. Conformational stability and DNA binding specificity of the cardiac T-box transcription factor Tbx20. *J Mol Biol* 2009;**389**:606—18.
14. **Coll M,** Seidman JG, Muller CW. Structure of the DNA-bound T-box domain of human TBX3, a transcription factor responsible for ulnar-mammary syndrome. *Structure* 2002;**10**:343—56.
15. **Stennard FA,** Costa MW, Elliott DA, Rankin S, Haast SJ, Lai D, McDonald LP, Niederreither K, Dolle P, Bruneau BG, Zorn AM, Harvey RP. Cardiac T-box factor Tbx20 directly interacts with Nkx2-5, GATA4, and GATA5 in regulation of gene expression in the developing heart. *Dev Biol* 2003;**262**:206—24.
16. **Hammer S,** Toenjes M, Lange M, Fischer JJ, Dunkel I, Mebus S, Grimm CH, Hetzer R, Berger F, Sperling S. Characterisation of TBX20 in human hearts and its regulation by TFAP2. *J Cell Biochem* 2008;**104**:1022—33.
17. **Ramensky V,** Bork P, Sunyaev S. Human non-synonymous SNPs: server and survey. *Nucleic Acids Res* 2002;**30**:3894—900.
18. **Ng PC,** Henikoff S. Predicting deleterious amino acid substitutions. *Genome Res* 2001;**11**:863—74.
19. **Posch MG,** Perrot A, Schmitt K, Mittelhaus S, Esenwein EM, Stiller B, Geier C, Dietz R, Gessner R, Ozcelik C, Berger F. Mutations in GATA4, NKX2.5, CRELD1, and BMP4 are infrequently found in patients with congenital cardiac septal defects. *Am J Med Genet A* 2008;**146A**:251—3.
20. **Hirayama-Yamada K,** Kamisago M, Akimoto K, Aotsuka H, Nakamura Y, Tomita H, Furutani M, Imamura S, Takao A, Nakazawa M, Matsuoka R. Phenotypes with GATA4 or NKX2.5 mutations in familial atrial septal defect. *Am J Med Genet A* 2005;**135**:47—52.
21. **Hagen PT,** Scholz DG, Edwards WD. Incidence and size of patent foramen ovale during the first 10 decades of life: an autopsy study of 965 normal hearts. *Mayo Clin Proc* 1984;**59**:17—20.
22. **Arquizan C,** Coste J, Touboul PJ, Mas JL. Is patent foramen ovale a family trait? A transcranial Doppler sonographic study. *Stroke* 2001;**32**:1563—6.
23. **Wilmshurst PT,** Pearson MJ, Nightingale S, Walsh KP, Morrison WL. Inheritance of persistent foramen ovale and atrial septal defects and the relation to familial migraine with aura. *Heart* 2004;**90**:1315—20.
24. **Biben C,** Weber R, Kesteven S, Stanley E, McDonald L, Elliott DA, Barnett L, Köentgen F, Robb L, Feneley M, Harvey RP. Cardiac septal and valvular dysmorphogenesis in mice heterozygous for mutations in the homeobox gene Nkx2-5. *Circ Res* 2000;**87**:888—95.
25. **Kirk EP,** Hyun C, Thomson PC, Lai D, Castro ML, Biben C, Buckley MF, Martin IC, Moran C, Harvey RP. Quantitative trait loci modifying cardiac atrial septal morphology and risk of patent foramen ovale in the mouse. *Circ Res* 2006;**98**:651—8.
26. **Postma AV,** van de Meerakker JB, Mathijssen IB, Barnett P, Christoffels VM, Ilgun A, Lam J, Wilde AA, Lekanne Deprez RH, Moorman AF. A gain-of-function TBX5 mutation is associated with atypical Holt-Oram syndrome and paroxysmal atrial fibrillation. *Circ Res* 2008;**102**:1433—42.